PSM
Biological Research

Research Article 2025 | Volume 10 | Issue 1 | 125-143

Open Access

Article Information

Received: November 28, 2025

Accepted: December 26, 2025

Published: December 31, 2025

Keywords

Mango,
ZnO NPs,
XRD,
Antioxidants,
In vivo activity,
Antidiabetic potential.

Authors' Contribution

SR conceived and designed the study; SA, TK, and MA conducted experiments; SA did statistical analysis; SA, MIS, and SR wrote and revised the paper.

How to cite

Akhtar, S., Kanwal, T., Ahmad, M., Shahzad, M.I., Rubnawaz, S., 2025. Synthesis, Characterization, and Biological Assessment of Zinc Oxide Nanoparticles using Azeem Chaunsa Mango Leaves. PSM Biol. Res., 10(1): 125-143.

***Correspondence**

Samina Rubnawaz
Email:
samina.rubnawaz@iub.edu.pk

Synthesis, Characterization, and Biological Assessment of Zinc Oxide Nanoparticles using Azeem Chaunsa Mango Leaves

Saba Akhtar[1], Tahreem Kanwal[1], Muneer Ahmad[1], Mirza Imran Shahzad[1], Samina Rubnawaz[*1]

[1]Department of Biochemistry & Molecular Biology, Institute of Biochemistry, Biotechnology, and Bioinformatics (IBBB), Faculty of Chemical & Biological Sciences, The Islamia University of Bahawalpur, Pakistan.

Abstract:

The advent of modern nanotechnology led to the development of zinc oxide nanoparticles (ZnO NPs) with a variety of commercial applications, including biomedical and therapeutic benefits. *Mangifera Indica* L. (mango), a tropical and subtropical fruit plant belonging to the Anacardiaceae family, is known as "the king of fruits" for its delicious taste and nutritional value. In this study, we used mango leaves of the Azeem Chaunsa variety to synthesize therapeutically important NPs. Here, the synthesis of ZnO NPs was confirmed by the UV-Visible spectra, while FTIR was used to determine the NPs' chemical composition and functional groups. X-ray diffraction (XRD) analysis revealed the formation of pure hexagonal ZnO NPs (6.2 nm). Phytochemical studies confirmed higher total phenolic (6.75±0.136 µg GAE/mg of dry weight) and flavonoid (5.77±3.94 µg QE/mg of dry weight) contents in NPs. Moreover, NPs demonstrated significant antioxidant potential, as evidenced by DPPH radical scavenging activity, reducing power, and total antioxidant content. Furthermore, the NPs exhibited better antibacterial activity against *Proteus vulgaris* (9.25±0.94 mm zone of inhibition) and antifungal activity against *Aspergillus flavus* (9.26±0.93 mm) compared to other tested strains. Additionally, our NPs significantly inhibited the activity of α-amylase enzyme *in vitro*. Female albino rats were used to examine the potential anti-inflammatory, analgesic, and antidiabetic properties of NPs and extracts *in vivo,* where NPs fared better than the extract. These outcomes ensured that our synthesized NPs can serve as a source of innovative nanomedicine to treat several diseases.

Scan QR code to visit this journal.

INTRODUCTION

Nanotechnology has made remarkable strides in recent years, with various effective techniques for creating nanoparticles (NPs) of specific sizes and shapes, which are utilized for particular applications (Ramesh *et al.*, 2015). Usually, NPs are smaller than 100 nm, possessing exceptional thermal stability, a high surface-to-volume ratio, and remarkable mechanical, electrical, magnetic, and electronic properties (Iftikhar *et al.*, 2019; Yousuf *et al.*, 2019). Therapeutic uses of nanoscale materials are diverse, encompassing drug delivery, disease diagnosis, and medical imaging (Ramesh *et al.*, 2015). Moreover, the ability of NPs to cross the gap between atomic or molecular structures and bulk materials makes them extremely interesting research material (Thakkar *et al.*, 2010). Metal and metal oxide NPs have been used in large-scale applications, which is a new trend that has emerged recently. Because of its unique optical and electrical properties, zinc oxide (ZnO), a long-lasting, more stable, and multifunctional metal oxide, is regarded as one of the best metal oxides that can be used for the synthesis of NPs (Abdul Salam *et al.*, 2014). With their wide bandwidth and high exciton binding energy, ZnO NPs demonstrate strong antibacterial, antifungal, antioxidant, anti-inflammatory, analgesic, and antidiabetic properties. ZnO NPs also exhibit the highest toxicity against microorganisms among all metal oxide NPs (Siddiqi *et al.*, 2018).

There are several methods for creating NPs, including physical, chemical, and biological methods. Experimental conditions and procedures influence the size and shape of NPs, including time, speed, chemical composition, and reaction temperature (Dastan, 2017). ZnO NPs synthesized from physical methods are mostly utilized in industrial processes and are produced at relatively high rates (Naveed Ul Haq *et al.*, 2017). Chemical synthesis involves creating metal NPs through one or more chemical processes (Srujana and Bhagat, 2022). Biological processes, also known as green chemistry, are simpler and offer greater potential, as they are more economical, adaptable, and environmentally acceptable, producing non-toxic, biodegradable NPs. This technology uses medicinal plants, algae, fungi, yeast, and enzymes to produce NPs (Narayana *et al.*, 2018). Plants and plant extracts offer a desirable platform for the synthesis of NPs, as several primary and secondary metabolites, including tannins, starches, polyphenols, flavonoids, terpenoids, and polypeptides, are present in plants that serve as effective capping and reducing agents (Khan *et al.*, 2016).

Mango or *Mangifera indica L.* (family Anacardiaceae) is a fruity plant that thrives all over the world in tropical and subtropical regions. Mangoes, often known as "the king of fruits," are the national fruit of Pakistan, India, Bangladesh, the Philippines, and many countries of the region (Mirza *et al.*, 2021). The plant is utilized to treat a variety of diseases, including cough, asthma, rheumatism, bronchitis, diarrhea, dementia, piles, hemorrhage, and hypertension (Saleem *et al.*, 2019). Its leaves, bark, flowers, roots, and fruits have been used to make antiseptic, dentifrice, diaphoretic, astringent, stomachic, vermifuge, laxative, and diuretic agents (Shahzad *et al.*, 2017).

Although plant-mediated synthesis of ZnO NPs has garnered considerable attention, a significant gap remains in understanding the role of specific plant extracts in tailoring the properties of NPs for multifunctional applications. This is the first study to explore the green synthesis of ZnO NPs using Azeem Chaunsa leaf extracts, leveraging its unique phytochemical profile and resultant antioxidant and antimicrobial properties. The work further investigates the *in vivo* anti-inflammatory, analgesic, and antidiabetic potential of synthesized nanoparticles.

MATERIALS AND METHODS

Collection of Plants and Extract Preparation

The fresh leaves of the *M. Indica* Azeem Chaunsa variety were collected from Bahawalpur, Pakistan. Plant sample was submitted to the departmental herbarium (IUB/Bot/Herb 615), and verified by Dr. Ghulam Sarwar, from the Department of Botany, the Islamia University of Bahawalpur. The collected leaves were washed with tap water and shade-dried for 15 days. Using a mixer and grinder, the dried leaves were processed until a coarse powder was formed. 15 g of powdered leaves were soaked in 100 ml of ethanol at room temperature for a day and then filtered with Whatman filter paper (Figure 1).

Fig. 1. Different steps in plant extract preparation for nanoparticles synthesis.

Synthesis of ZnO Nanoparticles

ZnO NPs were synthesized using *M. indica* leaves according to the following previously published protocol (MuthuKathija *et al.*, 2023), with slight modifications. Here, 0.1M zinc sulphate was dissolved in 50 ml of deionized water and continuously stirred at room temperature for 15 min. Next, 20 ml of freshly prepared leaf extract solution was mixed with this zinc sulfate solution. The resulting mixture was vigorously whirled in a magnetic stirrer for 2 hours at 70 °C. The resulting precipitate was allowed to settle after the reaction was completed. This precipitate was isolated from the reaction mixture by centrifugation at 6000 rpm for 15 min. It was then washed several times with deionized water to eliminate any remaining impurities and dried in a hot air oven at 80 °C. The resulting ZnO NPs were finely powdered and stored in an airtight container (Figure 2).

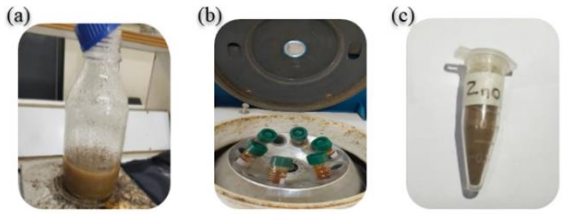

Fig. 2. ZnO NPs Synthesis **(a)** Reaction on Hot Plate **(b)** Centrifugation of Prepared Reaction Material **(c)** Synthesized ZnO NPs.

Characterization of ZnO NPs

Ultraviolet-Visible Spectroscopy

UV-visible spectroscopy was used to investigate the transmission, optical properties, and absorbance of ZnO NPs. The wavelength range of 200–800 nm was used to examine the UV spectrum and absorption (Narayana *et al.*,

2018). The specific absorbance was measured, and a standard peak was observed on a UV-Epoch- Biotek (USA) instrument.

FTIR

FTIR Spectroscopy was used for functional group identification and reduction potential using KBr pellets between 4000-500 cm^{-1} wavelength. This method confirms the reduction of the precursor and provides basic structural and functional characteristics (Narayana *et al.*, 2018). Characterization of NPs and their confirmation were performed using a Thomas Scientific FTIR analyzer at the Central Laboratory, Department of Chemistry, The Islamia University of Bahawalpur, Pakistan.

XRD

For describing the composition, size, and structure of various crystalline materials, XRD serves as a nondestructive and analytical approach. For this, X-rays are diffracted at normal angles in the lattice planes. The peak intensities reveal the distribution of atoms within a lattice. ZnO NPs' crystalline nature was verified by XRD at values between 10° and 70°. The ZnO NPs structure is indicated by the peak that appears at 2θ=36.21 (Khan *et al.*, 2019).

Phytochemical Assessment

For quantitative phytochemical analyses, the stock solutions of NPs and plant extracts were prepared in 10% DMSO.

Total Phenolic content (TPC) determination

The Total Phenolic Content (TPC) was determined using the Folin-Ciocalteu method (Jafri *et al.*, 2017). A stock solution of gallic acid standard (in 50% methanol), sodium carbonate (6%), and a 1:10 dilution of Folin-Ciocalteu reagent were prepared. For the assay, 100 µl of NPs and leaf extract were mixed with 150 µl Folin-Ciocalteu reagent, and incubated at 25 °C for 5 min, followed by the addition of 100 µl sodium carbonate. After 90 minutes, absorbance was measured at 750 nm. 10% DMSO served as a negative control, while gallic acid (200–1000 µg/ml) was used as a positive control. Experiments were performed in triplicate, and results were calculated using a calibration curve ($Y = 0.1908x – 0.1709$, $R^2 = 0.9928$). The formula is given as:

$C = V/m \times$ dilute factor

The corresponding amount of gallic acid, as established by the calibration curve, is represented by V, while C is used for TPC (µg GAE/mg of dry weight) and m is the weight of the sample.

Total Flavonoid content (TFC) determination

The Total Flavonoid Content (TFC) was determined using the aluminum chloride method (Jafri *et al.*, 2017). For the assay, 100 µl of NPs and leaf extract were mixed with 150 µl aluminum chloride (10%), 150 µl sodium acetate (1M), and 600 µl of 10% DMSO, followed by 45 min incubation at 25 °C. Absorbance was measured at 415 nm. 10% DMSO was the negative control, while quercetin (200–1000 µg/ml) was the positive control. Experiments were performed in triplicate, and results were calculated using a calibration curve ($Y = 0.147x – 0.2617$, $R^2 = 0.8733$) with the formula.

$C = V/m \times$ dilute factor

The corresponding amount of quercetin, as established by the calibration curve, is represented by V, while C is used for TFC (µg QE/mg of dry weight), and m is the weight of the sample.

Antioxidant Assays

DPPH free radical scavenging assay

The DPPH free radical scavenging assay was performed by using 4% DPPH stock solution prepared in methanol (Rubnawaz *et al.*, 2021). Ascorbic acid (1 mg/ml in 10% DMSO) was used as a positive control, 10% DMSO as a negative control, while the samples' stock solution was prepared as 4 mg/ml in 10% DMSO. The experiment used different concentrations of NPs and leaf extracts (125 to 1000 µl) dissolved in 1 ml freshly prepared DPPH solution and kept in the dark at room temperature for 30 minutes, and then absorbance was measured at 517 nm.

The % DPPH scavenging activity was calculated using the formula:

% scavenging = Abs control - Abs sample / Abs control × 100

Reducing power assay

The following approach was used for reducing the power assay (Rubnawaz *et al.*, 2021). We prepared phosphate buffer (0.2M, pH 6.6) along with potassium ferricyanide (1%), trichloroacetic acid (10%), and ferric chloride (1%). Again, a 4mg/ml stock solution of test samples was prepared as previously. The working mixture contained 0.5 ml of phosphate buffer and 2.5 ml of potassium ferricyanide, which was mixed with NPs and leaf extracts, and incubated at 50°C for 20 minutes, followed by centrifuging at 3000 rpm for 10 minutes. Then, 0.5 ml of supernatant was mixed with 0.5 ml trichloroacetic acid, 1 ml DMSO, and 0.2 ml ferric chloride, and the absorbance was measured at 700 nm. Here, 10% DMSO was the negative control, while ascorbic acid was the reference. Reducing power was calculated using a specific formula:

Reducing power activity (µg AAE/mg sample) = C × V / m

C is the concentration of ascorbic acid equivalent (AAE) from the calibration curve. V is the volume of extract, and m is the mass of the sample.

Total antioxidant content

The phosphor-molybdenum assay was performed to check the TAC of the tested samples. The reagent solution was prepared by mixing sulfuric acid (0.6M), sodium phosphate (28 Mm), and ammonium molybdate (4 mM) in distilled water (Rubnawaz *et al.*, 2021). NPs and leaves extract solutions received 1 ml reagent treatment, which underwent 90-minute incubation at 95°C in a water bath. When the solution cooled down to room temperature, absorbance was taken at 765 nm by using a spectrophotometer with ascorbic acid as a standard. Antioxidant activity was calculated using the given formula:

TAC (µg AAE/mg sample) = C × V / m

C is the concentration of ascorbic acid equivalent (AAE) from the calibration curve. V is the volume of extract, and m is the mass of the sample.

Antimicrobial Activity

Antimicrobial activity was performed according to the following protocol (Chandrasekaran *et al.*, 2022).

Antibacterial activity

To assess the antibacterial effects of leaf extracts and NPs, gram-positive and negative bacterial strains, including *Escherichia coli*, *Staphylococcus aureus*, *Proteus vulgaris, Klebsiella pneumoniae,* and *Fecal coliform,* were used. The preparation of nutrient agar began with dissolving 8 g in 300 ml of distilled water, followed by autoclaving. The prepared agar solution was poured into sterile petri dishes, which subsequently solidified. The bacterial cultures (200 µl) were spread on agar plates through a glass rod spreader. Then, 10 mg/ml leaf extracts and NPs were applied onto 5 mm sterile filter paper discs placed in the agar plates. The plates were incubated at 37°C for 24 hours, and then zones of inhibition were measured (Aernan *et al.*, 2024; Hussain *et al.*, 2016; Iqbal *et al.*, 2016). Here, Oxytetracycline (10mg/ml distilled water) was the positive control, whereas a 10% DMSO solution was the negative control, and the experiment was performed in triplicate.

Antifungal activity

The antifungal activity of the samples was evaluated using four fungal strains: *Aspergillus niger, Craterellus tubaeformis, Candida albicans,* and *Aspergillus flavus*. The assay was conducted on Potato Dextrose Agar (PDA) medium, prepared by dissolving 10 g glucose, 2.5 g peptone, and 4.5 g nutrient agar in 200 ml of distilled water, followed by autoclaving for sterilization. Agar plates were prepared by pouring 20 ml of the medium into each petri dish and allowing solidification. A fungal suspension (200 µl) was spread onto the plates using a spreader. Then, 10 mg/ml leaf extracts and NPs were applied onto sterile filter paper discs (5

mm) placed on the agar plates. The culture plates were incubated at 37 °C for 48 hours. After incubation, antifungal activity was assessed by measuring the zones of inhibition around the discs, indicating fungal growth suppression (Kabbashi and Al Fadhil, 2016; Kalim *et al.*, 2016; Kebede and Shibeshi, 2022). The results were compared between the leaf extract and NPs to determine their relative efficacy. Tineacort served as the positive control, while DMSO was used as the negative control.

α-Amylase inhibitory activity

The following protocol was used to perform the α-amylase inhibition activity (Mahmood et al., 2020). A solution of 0.005 g α-amylase was prepared in 100 ml of ice-cold distilled water, and ZnO NPs were added at concentrations of 250, 500, and 1000 µg/ml. Similar dilutions were prepared with extracts and tested alongside NPs for comparative analysis. To prevent NPs aggregation, the samples were sonicated for 30 minutes at room temperature. The reaction was allowed to proceed for 20 minutes, after which 2 ml of DNS reagent (1% dinitro-salicylic acid in 0.4 M NaOH) and sodium potassium tartrate (12%) were added. The mixture was then heated at 100 °C for 15 minutes. The absorbance was recorded at 540 nm, and enzyme inhibition was calculated accordingly:

% Inhibition α-Amylase = Abs control - Abs sample / Abs control × 100

In vivo Experiments

Experimental animals and study approval

Healthy female albino rats weighing between 100 and 120 g were used in this study. The experiments were performed in the Animal House of the Cholistan Institute of Desert Studies, the Islamia University of Bahawalpur, Pakistan. Animals were kept in a standard laboratory environment with a 12-hour light/dark cycle and a humidity range of 35-60%, as well as the full supply of regular food and water, as per the guidelines provided by the OECD (Organization for Economic Cooperation and Development). Animals weren't fed or provided with water before the experiment. Moreover, the study was approved by the Office of Research, Innovation and Commercialization (ORIC) Institutional Animal Ethics Committee (262/ORIC), and Institutional Bio-Safety Committee (270/ORIC), the Islamia University of Bahawalpur.

Anti-Inflammatory Activity

The assay for carrageenan-induced inflammation was carried out using previously published methodologies (Bhowmick *et al.*, 2014). For this, we used five distinct animal groups, each containing three rats (Table 1).

Table 1. Experimental Design of Anti-Inflammatory Activity.

Groups	Treatment
1st group	Normal control (Normal saline 5 ml/kg BW)
2nd group	Positive control (Carrageenan + Diclofenac 15 mg/kg BW)
3rd group	Negative control (Carrageenan + Normal Saline 5 ml/kg BW)
4th group	Carrageenan induced + NPs (200 mg/kg BW)
5th group	Carrageenan induced + Leaves extract (200 mg/kg BW)

BW is used for body weight, and NPs for nanoparticles.

Here, the 1st group received normal saline as a 5 ml/kg treatment, the 2nd and 3rd groups received diclofenac sodium as a 15 mg/kg standard treatment, and carrageenan with normal saline 5 ml/kg as a reference treatment, respectively. We injected diclofenac sodium injection as a standard drug, followed by a 30-minute interval to proceed with NPs administration through the oral route at 200 mg/kg BW in the fourth treatment group. An oral administration of a leaf extract (200 mg/kg BW) was used to assess its anti-inflammatory properties as part of the 5th group experiment. Paw sizes of all animals were measured at 1-, 2-, 3-, and 4-hour intervals following carrageenan injection. The % of inhibition (anti-inflammation) was then determined using the following formula:

$$\% \text{ inhibition} = N - N_t / N \times 100$$

(N = Paw size of the control group) (N_t = Paw size of treatment group)

Analgesic activity by the tail immersion test

The purpose of the experiment is to evaluate the given drug's analgesic potential and pain threshold. Here, the tail was left hanging while rats were placed into separate cylindrical carriers. Rats were divided into four groups (Table 2) with three rats in each group. The lower portion of the tail was marked up to 4-5 cm. 1st group was injected with normal saline (5ml/kg), in 2nd group, the standard drug (Paracetamol, 10 mg/kg) was injected intraperitoneally, 3rd group had oral administration of NPs (200 mg/kg), and in 4th group, the leaves extract 200mg/kg were given orally. After a 30-minute of treatment, the designated area of the tail was submerged in freshly filled warm water (55 °C). A stopwatch with an accuracy of 0.5 seconds was used to record the reaction time. The tail's withdrawal from the heat (flicking response) was considered the endpoint. To prevent damage to the tail, a 15-second cutoff time was maintained. Upon determining the response, the tail was thoroughly dried. Examined the tail-flick response at 30, 60, and 120 minutes. The flicking reaction, which measures the duration required to remove the tail from the hot water source, was measured, and the outcomes were compared with a normal control group (Wang *et al.*, 2020).

Table 2. Analgesic Activity by Tail Immersion Test.

Groups	Treatment
1st group	Normal control (Normal saline 5 ml/kg BW)
2nd group	Positive control (Paracetamol 10 mg/kg BW)
3rd group	NPs (200 mg/kg BW)
4th group	Leaves extract (200 mg/kg BW)

BW is used for body weight and NPs for nanoparticles.

Anti-Diabetic Activity in Alloxan-Induced Diabetic Rats

Anti-diabetic potential was assessed using the alloxan-induced diabetes animal models. The experiment was conducted on female albino rats with a body weight of 100-120 g, following the standard methodology (Chandrasekaran *et al.*, 2022). For this, alloxan monohydrate (98%) solution was prepared in normal saline, and injected intraperitoneally to induce diabetes in all rats (200 mg/kg) except the normal control group. In order to reduce early hyperglycemia, animals were then provided free access to feed and 5% dextrose solution water. After 72 hours of alloxan injection, a glucometer was used to measure the blood glucose levels. For this experiment, only the rats whose blood glucose levels were greater than 150 mg/dl were considered. Five groups of diabetic rats were formed, with three rats in each group, and oral treatments were given as detailed in Table 3.

Table 3. Experimental Design of Anti-Diabetic Activity.

Groups	Treatment
1st group	Normal control (Normal saline 5 ml/kg BW)
2nd group	Negative control (Alloxan + Normal Saline 5 ml/kg BW)
3rd group	Positive control (Alloxan + Glibenclamide 5 mg/kg BW)
4th group	NPs 200 mg/kg BW + alloxan induced
5th group	Leaves extract (200 mg/kg BW) + alloxan induced.

BW is used for body weight and NPs for nanoparticles.

RESULTS AND DISCUSSION

Characterization of NPs

Ultraviolet-visible spectroscopy

ZnO NPs and plant extract were observed by a visible spectrometer. The wavelength range of 200–800 nm was used to examine the UV spectrum and absorption. ZnO NPs indicated a notable peak at 450 nm (Figure 3). Moreover, plant extracts (control) showed no such peak.

Our results are further supported by previous studies that show ZnO NPs UV absorption spectra with an absorption peak in the range of 300–450 nm (Alrubaie and Kadhim, 2019). In another study, the ZnO NPs synthesized from mango seed extract showed a distinctive absorption spectrum at 480 nm, which proved the formation of ZnO NPs (Mohammadian *et al.*, 2018).

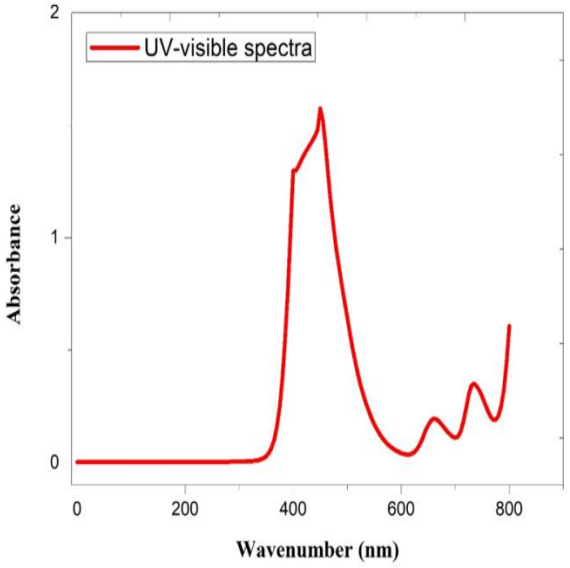

Fig. 3. UV-Visible Absorption Spectrum.

FTIR analysis

To identify the hidden organic functional groups and inorganic sites involved in the capping of the reducing agents, biosynthesized NPs were studied using FTIR spectroscopy. Utilizing plant-mediated particles with KBr pellets, FTIR analysis was conducted at normal temperature, FTIR spectrum was obtained in the wavenumber range 4000-500 cm^{-1}. Effectively copped over ZnO NPs, phytochemicals revealed some significant functional groups. Numerous peaks in the NPs' FTIR spectrum suggested the presence of complex organic compounds in the sample. In our study, the spectrum/band found at 3450 cm^{-1} suggests the existence of an O-H connection. The presence of a C-O bond is shown by the other signal at 2340 cm^{-1}, while signal at 1630 cm^{-1} confirms the presence of a C=C bond. The peak at 1110 cm^{-1} reveals the existence of ZnO NPs (Figure 4). The presence of ZnO salt in the sample is indicated by the distinct, well-defined band in the FTIR spectra at 500–600 cm^{-1}. Most metal oxides showed absorption between 400-600 wavenumbers. The findings show that the Zn precursor was strongly capped by the reducing agent of the plant extracts (Resmi *et al.*, 2021).

Earlier, many FTIR investigations validated the presence of these functional groups in *M. indica*. In one study, ZnO NPs from *M. indica* leaf extract showed an extensive variety of bands in the FTIR spectra at 3415, 3442, 1638, 1627 cm^{-1}, which are associated with the hydroxyl O-H group and signify the secondary metabolites. The peaks at 2916 and 2929 cm^{-1} illustrated the indication of alkane –CH elongation. The C=C conjugated groups were found at 2552 and 2341 cm^{-1}, where there is a slight depression surface. The emergence of peaks at 1638 and 1627 cm^{-1} expressing the C-O ester group and a peak at 739 cm^{-1} exhibiting N=O nitro group, signifies the availability of phytochemicals (Panwar *et al.*, 2022).

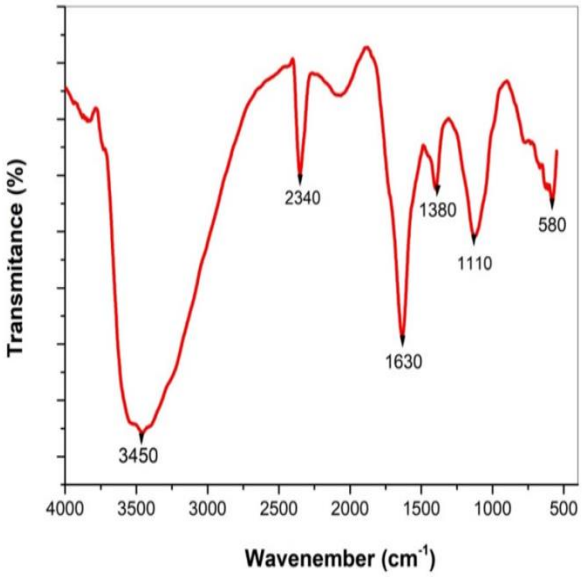

Fig. 4. FTIR Spectra of NPs.

XRD analysis

The ZnO NPs crystalline shape was identified by XRD pattern (Figure 5). In our study, ZnO NPs exhibit prominent and powerful peaks at 2θ 31.75°, 34.38°, 36.21°, 47.48°, 56.54°, and 67.87° along with the associated planes at (100), (002), (101), (102), (110), (103), (112). The existence of a peak at 2θ 36.21° confirms the synthesis of ZnO NPs. Cell parameters a=3.253Å and c=5.213Å of NPs demonstrated that particles are hexagonal in shape. Using Scherrer's formula, the crystalline size of NPs was determined to be 6.2 nm. In one study, the hexagonal Wurtzite

crystalline structure of the NPs was demonstrated by XRD peaks found at 2θ values 31.86°, 34.72°, 36.57°, 47.66°, 56.89°, 61.74°, and 68.69°. These peaks correlate to the lattice planes (100), (002), (101), (102), (110), (103), and (112) according to the JCPDS no. 36-1451. The existence of NPs is shown by lattice planes (100), (002), and (101) (Rajeshkumar *et al.*, 2018).

In another study, the 2θ distinctive peaks of ZnO NPs were identified by XRD at 31.60°, 34.22°, 36.11°, 47.35°, 56.45°, and 62.69° within the (100), (002), (101), (102), (110), and (103) planes of the crystal lattice, respectively. These peaks suggested the presence of the hexagonal Wurtzite type of ZnO NPs and were consistent with the standard JCPDS no. 89-0510 (Barzinjy and Azeez, 2020).

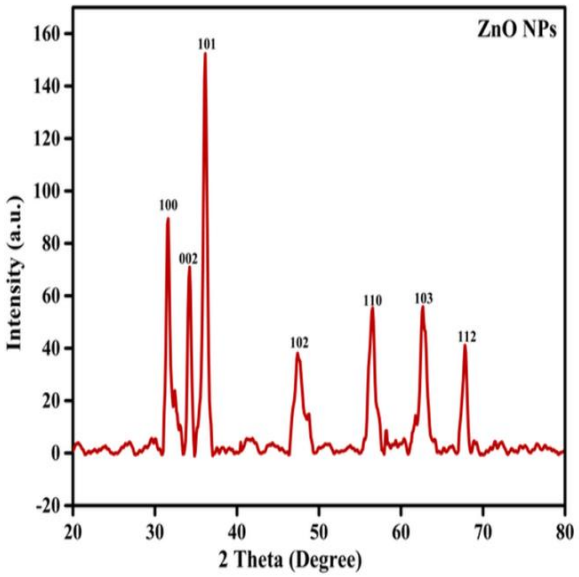

Fig. 5. The hexagonal Wurtzite crystalline structure of the NPs demonstrated by XRD peaks.

Phytochemical Analyses

Total phenolic and flavonoid content

All plants contain secondary metabolites, including phenolics and flavonoids with strong antioxidant activity. Phenolic compounds have hydroxyl groups that directly contribute to their antioxidant potential and act as scavengers of free radicals. As they are efficient hydrogen donors, phenolic compounds are also potent antioxidants (Kashkouli *et al.*, 2018). In the current study, *M. indica* leaf extract and NPs demonstrated a significant amount of total phenolic and flavonoid content. NPs exhibited a higher TPC (6.75 µg GAE/mg) and TFC (5.77 µg QE/mg), indicating a richer phenolic and flavonoid composition compared to the leaves extract with a TPC value of 3.40 µg GAE/mg and TFC of 2.71 µg QE/mg, suggesting a relatively lower antioxidant potential (Table 4).

In one report, the aqueous mango seed extract's qualitative phytoconstituent revealed the presence of terpenoids, polyphenols, flavonoids, and tannins, which may be contributing to its biological effects. The phytochemicals may also be responsible for the reduction of zinc ions to zinc oxide, which in turn facilitates the creation of NPs (Rajeshkumar *et al.*, 2023). Moreover, glycosides, flavonoids, tannins, phenols, coumarins, and anthocyanins were detected in the aqueous and methanol extracts of *M. indica* seed powder. The qualitative phytochemical analysis also identified these compounds in the seed powder (Donga *et al.*, 2020). Another study reported the TPC of 19.31±0.41 mg GAE/g extract, whereas the TFC of 22.06±1.74 mg QE/g extract in the ethanolic extract of mango peel exhibited (Wigati and Pratoko, 2024). These differences may be due to the differing solubility of metabolites in various solvent systems.

Table 4. Total Phenolic and Flavonoid Content.

Sample	TPC (µg GAE/mg of dry weight)	TFC (µg QE/mg of dry weight)	t-value	p-value
NPs.	6.75±0.136	5.77±3.94	2.34	0.042*
Leaf extracts	3.40 ± 0.79	2.71 ± 1.66	1.56	0.152

Values are presented as mean±SD (Standard deviation). This experimental data with the t-test does so in triplicate form. The asterisk (*) signifies statistical significance. A p-value below 0.05 ($p < 0.05$) indicates a significant value.

In vitro Antioxidant Assays

DPPH free radical scavenging activity

When evaluating a substance's potential for antioxidants, the DPPH is often utilized. The ability of antioxidants to scavenge free radicals is evaluated, with a focus on the stable DPPH radical that causes a solution to turn deep violet. Both the π system and an unpaired electron in the nitrogen atom are present in DPPH. Molar absorptivity is increased by substitution on the aromatic ring, and this effect is more pronounced if a substitute lengthens the conjugation (Das *et al.*, 2013).

Here, our nanoparticles showed better scavenging activity and an IC_{50} of 210.7±1µg/ml as compared to ascorbic acid (129.8±2 µg/ml). followed by leaf extracts (302.6±2 µg/ml (Table 5).

Table 5. DPPH IC50 value of NPs and leaves extract.

Sample	IC50 (µg/ml)	t-value	p-value
Ascorbic acid	129.8±2	1.31	0.006*
NPs	210.7 ± 1	2.78	0.012*
Leaves extract	302.6±2	3.12	0.023*

Values are presented as mean±SD (Standard deviation). Data are experimental; the t-test was used for statistical analysis. The asterisk (*) signifies statistical significance. A p-value below 0.05 ($p < 0.05$) indicates a significant value.

Moreover, the radical scavenging activity of all tested samples increased with an increase in the concentration from 125 to 1000 µg/ml, as shown in Figure 6. These findings suggest that using the plant extract for the synthesis of ZnO NPs enhanced its radical scavenging activity, which is in accordance with previous studies (Bharathi and Bhuvaneshwari, 2019); (Geetha and Thilakavathy).

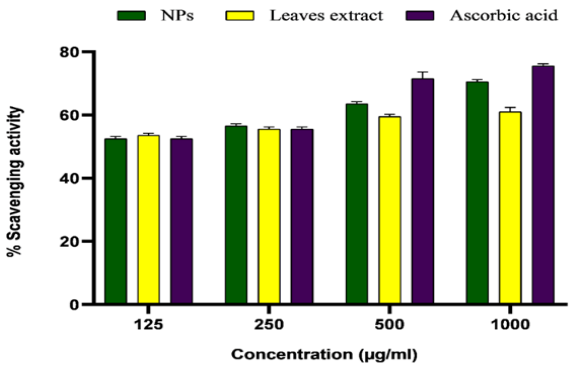

Fig. 6. DPPH Free Scavenging Activity of *M. indica* Leaves Extract and NPs.

Reducing power assay

The reducing power assay can be used to determine an antioxidant's electron-donating capacity. The assay's methodology involves first exposing samples to potassium ferricyanide (Fe^{3+}) to create potassium ferrocyanide (Fe^{2+}), and then exposing them to ferric chloride ($FeCl_3$) to create a ferric-ferrous complex (Alavi and Karimi, 2018).

Our results indicated that NPs exhibited reducing power activity of 61±13.8 µg AAE/mg of dry weight; similarly, leaf extracts showed reducing power activities of 67±12.06 µg AAE/mg of dry weight (Table 6). A previous study also suggested the potential reducing power of ZnO NPs and better antioxidant activity (Sohail *et al.*, 2020).

Table 6. Reducing Power Activity of NPs, Leaves Extract.

Sample	RPA (µg AAE/mg of dry weight)	t-value	p-value
NPs.	61±13.8	-2.393	0.027
Leaves extract	67 ± 12.06	-1.45	0.164

Values are presented as mean±SD (Standard deviation). The reducing power activities of the NPs and leaf extracts were evaluated and compared with those of ascorbic acid as a positive control. The asterisk (*) signifies statistical significance. A p-value below 0.05 ($p < 0.05$) indicates a significant value.

Phospho-molybdenum assay

The phosphor-molybdenum assay is a useful method for determining a substance's total antioxidant potential, which improves health, nutrition, and disease prevention studies (Inbathamizh *et al.*, 2013).

Our findings showed that NPs demonstrated total antioxidant activities of 74.50±6.455 µg AAE/mg of dry weight. Similarly, leaf extract demonstrated a total antioxidant capacity of 78.75±9.323 µg AAE/mg of dry weight. Thus, the leaf extracts showed a slightly higher value compared to NPs (Table 7).

A green phosphate-Mo (V) complex was formed at an acidic pH level because the sample reduced Mo (VI) to Mo (V), which served as the basis for the assay. In the reduction of phosphor-molybdenum complex, the Ag NPs also demonstrated strong antioxidant activity of 80±0.25 µg/ml as compared to the standard's 80±0.69 µg/ml activity (Inbathamizh *et al.*, 2013).

Table 7. Total Antioxidant Capacity of NPs and Leaf Extracts.

Sample	TAC (µg AAE/mg of dry weight)	t-value	p-value
NPs.	74.50±6.455	-2.496	0.021
Leaves extract	78.75 ± 9.323	-1.02	0.321

The total antioxidant capacities of the NPs and leaf extracts were assessed in comparison to ascorbic acid as a positive control. The asterisk (*) signifies statistical significance. A p-value below 0.05 ($p < 0.05$) indicates a significant value.

Antibacterial activity

The antibacterial activity of the synthesized NPs and the leaf extract was checked by using the disc diffusion method against gram-negative (*E. coli, F. coliform, K. pneumoniae, and P. vulgaris*) and gram-positive (*S. aureus*) bacterial strains. The maximal (9.25±0.94 mm) zone of inhibition was shown by NPs against *P. vulgaris,* whereas NPs were least (6.73±0.96 mm) active against *F. coliform.* In general, our NPs were found to have greater antibacterial action towards Gram-negative bacteria. Similarly largest zone of inhibition was shown by the leaves extract against *P. vulgaris* (12.96±0.97 mm), whereas the extracts were least effective against *F. coliform* with a zone of 9.33±0.7 mm (Table 8).

Previously, Ag NPs of *M. indica* exhibited potent antibacterial actions against *Bacillus subtilis*, *Pseudomonas fragi, E. coli, Streptococcus*, and *S. aureus, P. vulgaris,* and *Agalactiae* (Sarsar *et al.*, 2013).

In another study, ZnO NPs from *M. indica* peel aqueous extract were examined against three pathogenic bacteria. Gram-positive bacteria were more susceptible to the antibacterial properties of biosynthesized ZnO NPs than gram-negative bacteria. These ZnO NPs showed inhibitory zones of 8, 19, and 10 mm against *S. aureus, B. subtilis, and E. coli* (Endah *et al.*, 2023). Such antibacterial activity of ZnO NPs can be explained by their ability to bind to the cell walls of bacteria and cause membrane rupture, ultimately resulting in cell lysis (Slavin *et al.*, 2017).

Antimicrobial Potential

Table 8. Antibacterial Activity of samples.

Sample	Zone of inhibition (mm)						
	P. vulgaris	*F. coliform*	*K. pneumoniae*	*S. aureus*	*E. coli*	t-value	p-value
NPs.	9.25±0.94	6.73±0.9	9.16±0.93	7.73±0.08	-	2.45	0.035*
Leaves extract	12.96±0.97	12±0.91	11.63±0.94	12.06±0.89	9.33±0.7	3.01	0.011*
Oxytetracycline	22.3±0.7	22.1±0.9	15.3±0.87	19.4±0.96	20.7±0.8	-	-
DMSO 10%	-	-	-	-	-	-	-

Values are presented as mean±SD (Standard deviation). Experimental data was done in triplicate with a t-test. DMSO 10% was the negative control. Oxytetracycline (10mg/ml D.W) was the positive control. The asterisk (*) signifies statistical significance. A p-value below 0.05 ($p < 0.05$) indicates a significant value.

Moreover, Ag NPs synthesized from *M. indica* flower demonstrated antibacterial activity against three gram-negative bacteria *Rahnella sp*. *P. agglomerans* and *Klebsiella sp*. The percentage of inhibition obtained was 65.9%, 62.1% and 51.4%. Ag NPs' inhibitory properties have been linked to a breakdown of the cell membrane, which results in cytoplasm leakage and eventually cell death (Ameen *et al.*, 2019). Moreover, the potent antibacterial activity of AuNPs synthesized from *M. indica* seed extracts has also been reported against *S. aureus* and *E. coli* (Vimalraj *et al.*, 2018).

Antifungal activity

The antifungal activity of NPs and *M. indica* leaves extract was examined against *C. albicans, C. tubaeformis, A. niger, and A. flavus.* NPs demonstrated the largest inhibitory zone against *A. flavus* (9.26±0.93 mm), whereas the least (7.26±0.89 mm) activity against *C. albicans.* While extract shows the greatest possible inhibitory zone against *A. flavus* (10.96±0.96 mm), whereas least (6.63±0.99 mm) activity against *A. flavus* (Table 9).

Table 9. Antifungal Activity of NPs and Leaves.

Sample	**Zone of inhibition (mm)**					
	C. albicans	***C. tubaeformis***	***A. niger***	***A. flavus***	**t-value**	**p-value**
NPs.	7.26±0.89	7.63±0.94	7.3±0.94	9.26±0.93	2.67	0.025*
Leaves extract	6.73±0.96	8.96±0.752	10.96±0.96	6.63±0.99	2.89	0.018*
Tinea Cort	18.3±1.05	7.63±0.94	17.2±0.90	21.5±0.97	-	-
DMSO 10%	-	-	-	-	-	-

Values are expressed as mean±SD (Standard deviation). Experimental data is performed in a triplet form using a t-test. DMSO (10%) is used as a negative control. Tinea Cort (20mg/ml) is used as a positive control. The asterisk (*) signifies statistical significance. A p-value below 0.05 ($p < 0.05$) indicates a significant value.

Previously, ZnO NPs synthesized from multiple plant extracts have been reported to have antifungal activities (Al-darwesh *et al.*, 2024). Moreover, the antifungal potential of *M. indica* Ag NPs against *Stachybotrys chartarum* and *B. cereus* has also been well documented (Devi *et al.*, 2020). The presence of steroids, tannins, flavonoids, and phenols in *M. indica* leaves is thought to be responsible for their antimicrobial properties. These substances are effective antifungal and antibacterial agents, which may contribute to the antibacterial potential of *M. indica* (Mahalik *et al.*, 2017).

***In vitro* α-Amylase Inhibition activity**

The anti-diabetic potential of NPs and leaf extract was examined using the α-amylase inhibition assay. The results showed that, as the concentration of the NPs and the leaves extract increases, α-amylase inhibition activity increases. At varying doses of 250, 500, and 1000 µg/ml, the α-amylase inhibitory activity of NPs increased from 14.08% to 78.98%, and that of the leaves extract increased from 10.02% to 74.89% (Table 10). Here, the IC_{50} value for NPs was 210.6 ± 0.97 µg/ml, whereas that of the leaf extract was slightly higher at 225.4 ± 0.68 µg/ml. Acarbose showed a much lower IC_{50} value of 115.8 ± 0.86 µg/ml, indicating its greater inhibitory potency (Table 11).

The enzyme α-amylase breaks down α-α α-bonds in big linked polysaccharides like starch and glycogen to produce glucose and maltose. Preventing high postprandial blood glucose can be achieved in part by blocking this enzyme (Mechchate *et al.*, 2021).

Multiple studies have reported the inhibition of α-amylase enzyme by green-synthesized ZnO NPs in a concentration-dependent manner (Jeyaraj and Saral, 2024).

Table 10. α-Amylase Inhibitory Activity.

	α-amylase % inhibition				
Concentration (µg/ml)	**NPs**	**Leaves extract**	**Positive control (Acarbose)**	**t-value**	**p-value**
250	14.08%	10.02%	69.05%	2.34	0.042*
500	50.57%	45.21%	81.75%	3.01	0.011*
1000	78.98%	74.89%	90.53%	2.78	0.023*

Values are expressed as mean±SD (Standard deviation). Experimental data is performed in triplet form using one-way ANOVA. Acarbose is used as a positive control. The asterisk (*) signifies statistical significance. A p-value below 0.05 ($p < 0.05$) indicates a significant value.

Table 11. IC50 Value of NPs, Leaves Extract, and Acarbose.

Sample	**IC50 Value (µg/ml)**	**t-value**	**p-value**
NPs.	210.6±0.97	-126.7	< 0.001
Leaves extract	225.4 ± 0.68	-173.4	< 0.001
Acarbose	115.8±0.86	-	-

Values are expressed as mean±SD (Standard deviation). Experimental data is performed in triplet form using one-way ANOVA. Acarbose is used as a positive control. The asterisk (*) signifies statistical significance. A p-value below 0.05 ($p < 0.05$) indicates a significant value.

In vivo Activities

Anti-Inflammatory activity

The model of paw oedema caused by carrageenan is based on three stages of the inflammatory process. The hypothalamus releases prostaglandins throughout the early stages, at the site of inflammation, which induce vascular permeability. The later stage involves the activation of tissue macrophages to increase bradykinin and leukotriene levels (Wang *et al.*, 2014). Diclofenac sodium is a common drug that inhibits cyclooxygenase enzymes, which eventually results in a decrease in prostaglandin (Menasse *et al.*, 1978).

In our study following carrageenan-based inflammation in rats, observation was made at intervals of 1 to 4 hours. As a positive control, Diclofenac (15 mg/kg BW), a standard drug, considerably decreased inflammation in the rats' paws within the first hour. In the latter stage, it considerably contributes to the inflammation's reduction to a normal level by the 4th hour of inflammation. At a dose of 200 mg/kg BW, NPs showed a significant anti-inflammatory effect (Table 12). NPs slightly reduced inflammation within the 1st hour, with the highest impact in 4th hour (7.360±0.410 mm) when compared with the leaves extract group at a dose of 200 mg/kg BW (6.60±0.13 mm), and the negative control group showed a paw volume of 12.552±0.095 mm.

In an earlier report, the significant anti-inflammatory properties of Ag NPs were observed in an aqueous ethanolic bark extract of *M. indica* (Algarni *et al.*, 2023). A prior investigation demonstrated the anti-inflammatory properties of methanolic *M. indica* leaf extract, at doses of 200, 500, and 1000 mg/kg, using a carrageenan-induced acute rat paw edema approach (Sarkar, 2015).

Table 12. Anti-Inflammatory Potential of NPs and Extracts.

	Paw size (mm)						
Group Description	**0h**	**1h**	**2h**	**3h**	**4h**	**t-value**	**p-value**
1st group Normal control	6.5±0.01	6.41±0.1	6.4±0.005	6.41±0.01	6.29±0.05	-	-
2nd group Positive control	6.8±0.01	12.60±0.005	11.2±0.09	8.04±0.009	6.93±0.05	3.12	0.012*
3rd group Negative control	5.4±0.01	11.52±0.025	11.6±0.05	11.66±0.09	12.5±0.09	0.89	0.018*
4th group NPs.	6.16±0.12	11.62±0.672	11.1±0.5	9.30±0.21	7.36±0.41	2.67	0.025*
5th group Leaves Extract	6.32±0.21	12.25±0.172	10.140±0.16	8.00±0.18	6.60±0.13	2.45	0.035*

Values are expressed as mean±SD (Standard deviation). Experimental data is performed in triplet form using one-way ANOVA. Diclofenac (15mg/kg) is used as a positive control. Normal saline (5mg/kg) is used as a negative control. The asterisk (*) signifies statistical significance. A p-value below 0.05 ($p < 0.05$) indicates a significant value.

Analgesic Activity

Paracetamol (10 mg/kg) is used as a positive control in the tail immersion test and involves dipping the tip of the tail up to 5 cm in hot water, and recording the animal's response time (latency time) in seconds after the administration of a dose for 0, 30, 60, 90, and 120 min. Here, the response of tail withdrawal from hot water was noted. We observed that NPs and leaf extract reduced pain in a time-dependent manner. NPs' latency time increased from 0.940±0.071 sec (0 min) to 3.900±0.028 sec in (120 min), (Table 13). These results are compared with leaf extract, which is better than NPs, with a latency period of 1.124±0.21 sec to 4.60±0.13 sec during the same period.

Table 13. Analgesic Activity by Tail Immersion Test.

	Response time (sec)						
Group Description	**0 min**	**30 min**	**60 min**	**90 min**	**120 min**	**t-value**	**p-value**
1st group Normal control	1.32±0.015	1.55±0.04	1.66±0.02	1.22±0.01	1.49±0.16	-	-
2nd group Positive control	1.22±0.01	1.62±0.11	1.91±0.17	2.22±0.11	3.44±0.11	3.01	0.011*
3rd group NPs	0.94±0.07	1.21±0.12	1.93±0.72	3.34±0.72	3.9±0.02	2.78	0.023*
4th group Leaves Extract	1.124±0.21	1.45±0.172	2.140±0.16	3.90±0.18	4.60±0.13	2.34	0.042*

Values are expressed as mean±SD (Standard deviation). Experimental data is performed in triplet form using one-way ANOVA. Paracetamol (10mg/kg) is used as a positive control. Normal saline (5ml/kg) is used as a normal control. The asterisk (*) signifies statistical significance. A p-value below 0.05 ($p < 0.05$) indicates a significant value.

In earlier research, numerous *in vivo* and *in vitro* investigations have been carried out to look at the ZnO NPs' analgesic properties. The studies often demonstrate how ZnO NPs have a strong analgesic impact (Kesmati and Torabi, 2014). In the hot water tail immersion method, the ZnO NPs treated mice demonstrated an increase in reaction time in a dose-dependent manner (7.79 ± 0.82, 8.89 ± 0.82, 9.96 ± 0.74 sec, respectively), in contrast to the control (6.69 ± 0.13 sec). The reaction time reduced over time (Wang *et al.*, 2020).

Anti-Diabetic Activity

In this experiment, alloxan (200 mg/kg BW) was used to cause diabetes in rats. Glibenclamide was one of the drugs used to combat diabetes. Prior to the dosage being administered, the level of blood glucose was assessed. Consideration was given to animals whose blood glucose levels were greater than 150 mg/dl. When the NPs dosage was applied, the fasting blood sugar level started dropping significantly (210 mg/dl) after the 5th day, compared with negative control animals (230.3±54.85 mg/dl), but the extract group showed the most significant result

by decreasing the sugar level from 215.33±6.61 to 174.36±47.38. At the end of the experiment (13th day), NPs treated group had similar sugar levels (157±15.39 mg/dl) as the Glibenclamide-treated group (156.3±16.0 mg/dl), but when compared with the extract group, it showed less (136.3±16.0) than that of the NPs group (Table 14). However, these values were still significantly higher than the normal control group (77.0±6.55 mg/dl).

In one report, the oral hypoglycemic effects of absolute alcohol extracts of leaves and kernel seed of *M. indica* (100mg and 200mg/kg) were evaluated by glucose tolerance test. Administration of 200 mg/kg extracts produced a significant hypoglycemic impact in the fasted rats 3 hours post-treatment. Furthermore, both extracts also elevated insulin levels in alloxan-induced diabetic rats (Petchi *et al.*, 2011).

Table 14. Hypoglycemic Activity of NPs and Leaf Extracts in Alloxan-induced Diabetic Rats

Group Description	1st Day	7th Day	11th Day	13th Day	t-value	p-value
Normal control	79.33 ± 4.72	80.66 ± 305	75.3 ± 7.31	77.0 ± 6.55	-	-
Positive control	178.33 ± 56.61	166.66 ± 8.38	159.33 ± 17.0	156.3 ± 16.0	3.12	0.012*
Negative control	194.0 ± 104.50	233.66 ± 63.8	216.0 ± 37.32	238.33 ± 58.10	2.89	0.018*
NPs	210.0 ± 23.25	176.66 ± 14.57	160 ± 14.73	157 ± 15.39	2.67	0.025*
Leaves Extract	215.33 ± 6.61	166.66 ± 8.38	149.33 ± 17.0	136.3 ± 16.0	2.45	0.035*

Values are expressed as mean±SD (Standard deviation). Experimental data is performed in triplet form using one-way ANOVA. Glibenclamide (5mg/kg) is used as a positive control, and normal saline (5ml/kg) as a negative control. The asterisk (*) signifies statistical significance. A p-value below 0.05 ($p < 0.05$) indicates a significant value.

Potential antidiabetic effects of green-synthesized ZnO as well as Ag NPs have also been demonstrated in multiple other studies (Alkaladi *et al.*, 2014; Umrani and Paknikar, 2014) where ZnO NPs fared much better than the Ag counterparts.

Zinc used for ZnO NPs synthesis could account for the antidiabetic potential of nanoparticles. This trace metal affects several enzymatic activities and cellular processes, including increased insulin receptor phosphorylation, enhanced PI3K activity, inhibition of glycogen synthase kinase-3 (GSK-3), and improved insulin signaling in the body. Furthermore, its supplementation has been found to positively impact glycemic control in diabetic patients (Ahmed *et al*., 2022).

CONCLUSION

The green synthesis of ZnO NPs using *M. indica* leaf extract is reported in this study and verified by FTIR, XRD, and UV-Vis studies. Leaf extract and NPs demonstrated strong antioxidant, antibacterial, antifungal, and α-amylase inhibition properties, as well as noteworthy phytochemical content. They were shown to have analgesic, anti-inflammatory, and antidiabetic effects in *in vivo* experiments. These findings suggest ZnO NPs and leaf extract possess promising therapeutic applications, warranting further research.

These findings not only present a sustainable alternative for NPs synthesis but also open new possibilities for designing ZnO NPs with enhanced biological and environmental remediation potential.

CONFLICT OF INTEREST

The authors hereby declare that they have no conflict of interest.

REFERENCES

Abdul Salam, H., Sivaraj, R., Venckatesh, R., 2014. Green synthesis and characterization of zinc oxide nanoparticles from *Ocimum basilicum* L. var. purpurascens Benth.-Lamiaceae leaf extract. Mater. Lett., 131: 16-18.

Aernan, P.T., Odo, J.I., Ado, B.V., Mende, I.U., Yaji, E.M., Iqbal, M.N., 2024. Phytochemical and Antibacterial Assessment of *Ageratum conyzoides* Cultivated in Benue State, Nigeria. PSM Biol. Res., 9(1): 41-50.

Al-darwesh, M.Y., Ibrahim, S.S., Mohammed, M.A., 2024. A review on plant extract mediated green synthesis of zinc oxide nanoparticles and their biomedical applications. Results Chem., 101368.

Alavi, M., Karimi, N., 2018. Characterization, antibacterial, total antioxidant, scavenging, reducing power and ion chelating activities of green synthesized silver, copper and titanium dioxide nanoparticles using *Artemisia haussknechtii* leaf extract. Artif. Cells, Nanomed., Biotechnol., 46(8): 2066-2081.

Algarni, A., Fayomi, A., Al Garalleh, H., Afandi, A., Brindhadevi, K., Pugazhendhi, A., 2023. Nanofabrication synthesis and its role in antibacterial, anti-inflammatory, and anticoagulant activities of AgNPs synthesized by *Mangifera indica* bark extract. Environ. Res., 231: 115983.

Alkaladi, A., Abdelazim, A.M., Afifi, M., 2014. Antidiabetic activity of zinc oxide and silver nanoparticles on streptozotocin-induced diabetic rats. Int. J. Mol. Sci., 15(2): 2015-2023.

Alrubaie, E., Kadhim, R.E., 2019. Synthesis of ZnO nanoparticles from olive plant extract. Plant Arch., 19(2): 339-344.

Ameen, F., Srinivasan, P., Selvankumar, T., Kamala-Kannan, S., Al Nadhari, S., Almansob, A., Dawoud, T., Govarthanan, M., 2019. Phytosynthesis of silver nanoparticles using *Mangifera indica* flower extract as bioreductant and their broad-spectrum antibacterial activity. Bioorg. Chem., 88: 102970.

Barzinjy, A.A., Azeez, H.H., 2020. Green synthesis and characterization of zinc oxide nanoparticles using *Eucalyptus globulus* Labill. leaf extract and zinc nitrate hexahydrate salt. SN Appl. Sci., 2(5): 991.

Bharathi, D., Bhuvaneshwari, V., 2019. Synthesis of zinc oxide nanoparticles (ZnO NPs) using pure bioflavonoid rutin and their biomedical applications: antibacterial, antioxidant and cytotoxic activities. Res. Chem. Intermed., 45: 2065-2078.

Bhowmick, R., Sarwar, M.S., RahmanDewan, S.M., Das, A., Das, B., NasirUddin, M.M., Islam, M.S., Islam, M.S., 2014. In vivo analgesic, antipyretic, and anti-inflammatory potential in Swiss albino mice and in vitro thrombolytic activity of hydroalcoholic extract from *Litsea glutinosa* leaves. Biol. Res., 47: 1-8.

Chandrasekaran, S., Anusuya, S., Anbazhagan, V., 2022. Anticancer, anti-diabetic, antimicrobial activity of zinc oxide nanoparticles: A comparative analysis. J. Mol. Struct., 1263: 133139.

Das, D., Nath, B.C., Phukon, P., Dolui, S.K., 2013. Synthesis of ZnO nanoparticles and evaluation of antioxidant and cytotoxic activity. Colloids. Surf. B: Biointerfaces., 111: 556-560.

Dastan, D., 2017. Effect of preparation methods on the properties of titania nanoparticles: solvothermal versus sol–gel. Appl. Phys. A., 123: 1-13.

Devi, M., Devi, S., Sharma, V., Rana, N., Bhatia, R.K., Bhatt, A.K., 2020. Green synthesis of silver nanoparticles using methanolic fruit extract of *Aegle marmelos* and their antimicrobial potential against human bacterial pathogens. J. Tradit. Complement. Med., 10(2): 158-165.

Donga, S., Bhadu, G.R., Chanda, S., 2020. Antimicrobial, antioxidant and anticancer activities of gold nanoparticles green synthesized using *Mangifera indica* seed aqueous extract. Artif. Cells, Nanomed. Biotechnol., 48(1): 1315-1325.

Endah, E., Saraswaty, V., Ratnaningrum, D., Kosasih, W., Ardiansyah, A., Risdian,

C., Nugroho, P., Aji, E., Setiyanto, H., 2023. Phyto-assisted synthesis of zinc oxide nanoparticles using mango (*Mangifera indica*) fruit peel extract and their antibacterial activity, IOP Conference Series: Earth and Environmental Science. IOP Publishing, pp. 012081.

Geetha, S.U., Thilakavathy, S., Invitro DPPH Activity and Cytotoxicity Analysis of Zinc Oxide Nanoparticles (ZNONPS) From *Mangifera Indica* L. Anacardiaceae Leaves Extract. Int. J. Health Sci., 6(S5): 5285-5293.

Hussain, F., Kalim, M., Ali, H., Ali, T., Khan, M., Xiao, S., Iqbal, M.N., Ashraf, A., 2016. Antibacterial activities of methanolic extracts of *Datura inoxia*. PSM Microbiol., 1(1): 33-35.

Iftikhar, S., Warsi, M.F., Haider, S., Musaddiq, S., Shakir, I., Shahid, M., 2019. The impact of carbon nanotubes on the optical, electrical, and magnetic parameters of Ni^{2+} and Co^{2+} based spinel ferrites. Ceram. Int., 45(17): 21150-21161.

Inbathamizh, L., Ponnu, T.M., Mary, E.J., 2013. In vitro evaluation of antioxidant and anticancer potential of *Morinda pubescens* synthesized silver nanoparticles. J. Pharm. Res., 6(1): 32-38.

Iqbal, M.N., Ali, S., Anjum, A.A., Muhammad, K., Ali, M.A., Wang, S., Khan, W.A., Khan, I., Muhammad, A., Mahmood, A., 2016. Microbiological Risk Assessment of Packed Fruit Juices and Antibacterial Activity of Preservatives Against Bacterial Isolates. Pak. J. Zool., 48(6).

Jafri, L., Saleem, S., Ihsan ul, H., Ullah, N., Mirza, B., 2017. In vitro assessment of antioxidant potential and determination of polyphenolic compounds of *Hedera nepalensis* K. Koch. Arab. J. Chem., 10: S3699-S3706.

Jeyaraj, S., Saral, A.M., 2024. Bio-fabrication of zinc oxide nanoparticles from *Brassica juncea* (L.) Czern extract: Biological activity and DNA binding capability. Results. Chem., 101747.

Kabbashi, M.A., Al Fadhil, A.O., 2016. In vitro Antifungal Activity of Camel's Urine against Dermatophytes. Am. J. Res. Comm., 4(4): 183-191.

Kalim, M., Hussain, F., Ali, H., Ahmad, I., Iqbal, M.N., 2016. Antifungal activities of methanolic extracts of *Datura inoxia*. PSM Biol. Res., 1(2): 70-73.

Kashkouli, S., Jamzad, M., Nouri, A., 2018. Total phenolic and flavonoids contents, radical scavenging activity and green synthesis of silver nanoparticles by *Laurus nobilis* L. leaves aqueous extract. J. Med. Plants. By-prod., 7(1): 25-32.

Kebede, B., Shibeshi, W., 2022. In vitro antibacterial and antifungal activities of extracts and fractions of leaves of *Ricinus communis* Linn against selected pathogens. Vet. Med. Sci., 8(4): 1802-1815.

Kesmati, M., Torabi, M., 2014. Interaction between analgesic effect of nano and conventional size of zinc oxide and opioidergic system activity in animal model of acute pain. Basic. Clin.l Neurosci., 5(1): 80.

Khan, M.A., Khan, T., Nadhman, A., 2016. Applications of plant terpenoids in the synthesis of colloidal silver nanoparticles. Adv. Colloid. Interface. Sci., 234: 132-141.

Khan, Z.U.H., Sadiq, H.M., Shah, N.S., Khan, A.U., Muhammad, N., Hassan, S.U., Tahir, K., Khan, F.U., Imran, M., Ahmad, N., 2019. Greener synthesis of zinc oxide nanoparticles using *Trianthema portulacastrum* extract and evaluation of its photocatalytic and biological applications. J. Photochem. Photobiol. B., 192: 147-157.

Mahalik, G., Sahoo, S., Satapathy, K.B., 2017. Evaluation of phytochemical constituents and antimicrobial properties of *Mangifera indica* L. Leaves against

urinary tract infection-causing pathogens. Eval., 10(9): 169.

Mechchate, H., Es-Safi, I., Louba, A., Alqahtani, A.S., Nasr, F.A., Noman, O.M., Farooq, M., Alharbi, M.S., Alqahtani, A., Bari, A., 2021. In vitro alpha-amylase and alpha-glucosidase inhibitory activity and in vivo antidiabetic activity of *Withania frutescens* L. Foliar extract. Mol., 26(2): 293.

Menasse, R., Hedwall, P., Kraetz, J., Pericin, C., Riesterer, L., Sallmann, A., Ziel, R., Jaques, R., 1978. Pharmacological properties of diclofenac sodium and its metabolites. Scand. J. Rheumatol., 7(sup22): 5-16.

Mirza, B., Croley, C.R., Ahmad, M., Pumarol, J., Das, N., Sethi, G., Bishayee, A., 2021. Mango (*Mangifera indica* L.): a magnificent plant with cancer preventive and anticancer therapeutic potential. Crit. Rev. Food Sci. Nutr., 61(13): 2125-2151.

Mohammadian, M., Es'haghi, Z., Hooshmand, S., 2018. Green and chemical synthesis of zinc oxide nanoparticles and size evaluation by UV–vis spectroscopy. J. Nanomed. Res., 7(1): 00175.

MuthuKathija, M., Sheik Muhideen Badhusha, M., Rama, V., 2023. Green synthesis of zinc oxide nanoparticles using *Pisonia alba* leaf extract and its antibacterial activity. Appl. Surf. Sci. Adv., 15: 100400.

Narayana, A., Azmi, N., Tejashwini, M., Shrestha, U., Lokesh, S., 2018. Synthesis and characterization of zinc oxide (zno) nanoparticles using mango (*Mangifera indica*) leaves. Int. J. Res. Anal. Rev., 5(3): 432-439-432-439.

Naveed Ul Haq, A., Nadhman, A., Ullah, I., Mustafa, G., Yasinzai, M., Khan, I., 2017. Synthesis approaches of zinc oxide nanoparticles: the dilemma of ecotoxicity. J. Nanomater., 2017(1): 8510342.

Panwar, R.S., Pervaiz, N., Dhillon, G., Kumar, S., Sharma, N., Aggarwal, N., Tripathi, S., Kumar, R., Vashisht, A., Kumar, N., 2022. *Mangifera indica* leaf extract assisted biogenic silver nanoparticles potentiates photocatalytic activity and cytotoxicity. J. Mater. Sci.: Mater. Electron., 33(20): 16538-16549.

Petchi, R., Parasuraman, S., Vijaya, C., Girish Darwhekar, G.D., Devika, G., 2011. Antidiabetic effect of kernel seeds extract of *Mangifera indica* (Anacardiaceae). Int. J. Pharma. Bio Sci., 2(1): 385-393.

Rajeshkumar, S., Kumar, S.V., Ramaiah, A., Agarwal, H., Lakshmi, T., Roopan, S.M., 2018. Biosynthesis of zinc oxide nanoparticles using *Mangifera indica* leaves and evaluation of their antioxidant and cytotoxic properties in lung cancer (A549) cells. Enzyme Microb. Technol., 117: 91-95.

Rajeshkumar, S., Parameswari, R.P., Sandhiya, D., Al-Ghanim, K.A., Nicoletti, M., Govindarajan, M., 2023. Green synthesis, characterization and bioactivity of *Mangifera indica* seed-wrapped zinc oxide nanoparticles. Mol., 28(6): 2818.

Ramesh, M., Anbuvannan, M., Viruthagiri, G., 2015. Green synthesis of ZnO nanoparticles using *Solanum nigrum* leaf extract and their antibacterial activity. Spectrochim. Acta. A.: Mol. Biomol. Spectrosc., 136: 864-870.

Resmi, R., Yoonus, J., Beena, B., 2021. A novel greener synthesis of ZnO nanoparticles from *Nilgiriantus ciliantus* leaf extract and evaluation of its biomedical applications. Mater. Today.: Proc., 46: 3062-3068.

Rubnawaz, S., Kayani, W.K., Akhtar, N., Mahmood, R., Khan, A., Okla, M.K., Alamri, S.A., Alaraidh, I.A., Alwasel, Y.A., Mirza, B., 2021. Polyphenol Rich Ajuga bracteosa Transgenic Regenerants Display Better

Pharmacological Potential. Mol., 26(16): 4874.

Saleem, M., Tanvir, M., Akhtar, M.F., Iqbal, M., Saleem, A., 2019. Antidiabetic potential of *Mangifera indica* L. cv. Anwar Ratol leaves: medicinal application of food wastes. Med., 55(7): 353.

Sarkar, M., 2015. Evaluation of the anti-inflammatory activity of methanolic leaf extract of *Mangifera indica* L.(Anacardiaaceae) in rats. Int. J. Drug Dev. Res., 7(3).

Sarsar, V., Selwal, K.K., Selwal, M.K., 2013. Green synthesis of silver nanoparticles using leaf extract of *Mangifera indica* and evaluation of their antimicrobial activity. J. Microbiol. Biotech. Res., 3(5): 27-32.

Shahzad, M.I., Ashraf, H., Iqbal, M.N., Khanum, A., 2017. Medicinal Evaluation of Common Plants against Mouth Microflora. PSM Microbiol., 2(2): 34-40.

Siddiqi, K.S., ur Rahman, A., Tajuddin, n., Husen, A., 2018. Properties of zinc oxide nanoparticles and their activity against microbes. Nanoscale Res. Lett., 13: 1-13.

Slavin, Y.N., Asnis, J., Hńfeli, U.O., Bach, H., 2017. Metal nanoparticles: understanding the mechanisms behind antibacterial activity. J. Nanobiotechnol., 15: 1-20.

Sohail, M.F., Rehman, M., Hussain, S.Z., Huma, Z.-E., Shahnaz, G., Qureshi, O.S., Khalid, Q., Mirza, S., Hussain, I., Webster, T.J., 2020. Green synthesis of zinc oxide nanoparticles by Neem extract as multi-facet therapeutic agents. J. Drug Deliv. Sci. Technol., 59: 101911.

Srujana, S., Bhagat, D., 2022. Chemical-based synthesis of ZnO nanoparticles and their applications in agriculture. Nanotechnol. Environ. Eng., 7(1): 269-275.

Thakkar, K.N., Mhatre, S.S., Parikh, R.Y., 2010. Biological synthesis of metallic nanoparticles. Nanomedicine., 6(2): 257-262.

Umrani, R.D., Paknikar, K.M., 2014. Zinc oxide nanoparticles show antidiabetic activity in streptozotocin-induced Type 1 and 2 diabetic rats. Nanomedicine., 9(1): 89-104.

Vimalraj, S., Ashokkumar, T., Saravanan, S., 2018. Biogenic gold nanoparticles synthesis mediated by *Mangifera indica* seed aqueous extracts exhibits antibacterial, anticancer and anti-angiogenic properties. Biomed. Pharmacother., 105: 440-448.

Wang, Y., Zhao, G.-X., Xu, L.-H., Liu, K.-P., Pan, H., He, J., Cai, J.-Y., Ouyang, D.-Y., He, X.-H., 2014. Cucurbitacin IIb exhibits anti-inflammatory activity through modulating multiple cellular behaviors of mouse lymphocytes. PloS One., 9(2): e89751.

Wang, Z., Que, B., Gan, J., Guo, H., Chen, Q., Zheng, L., Marraiki, N., Elgorban, A.M., Zhang, Y., 2020. Zinc oxide nanoparticles synthesized from *Fraxinus rhynchophylla* extract by green route method attenuates the chemical and heat induced neurogenic and inflammatory pain models in mice. J. Photochem. Photobiol. B., 202: 111668.

Wigati, D., Pratoko, D.K., 2024. Study of Antioxidant Activity, Total Phenolic Content (TPC), and Total Flavonoid Content (TFC) of Ethanolic Extract Mango Peel (*Mangifera indica* L.). J. Sains. Kes., 6(1): 142-148.

Yousuf, M.A., Baig, M.M., Waseem, M., Haider, S., Shakir, I., Khan, S.U.-D., Warsi, M.F., 2019. Low cost micro-emulsion route synthesis of Cr-substituted $MnFe_2O_4$ nanoparticles. Ceram. Int., 45(17): 22316-22323.